

# Sintering study of ITO using a ZnO-doped and microwave hybrid sintering approach

Di Chen, Chongxi Jiang, Hongliang Sun, Bo Feng, Xiong Lu, Jie Weng, Jianxin Wang\*

Key Laboratory of Advanced Technologies of Materials, Ministry of Education, School of Materials Science and Engineering, Southwest Jiaotong University, Chengdu 610031, People's Republic of China

## ARTICLE INFO

### Article history:

Received 24 October 2013

Received in revised form

10 December 2013

Accepted 8 January 2014

Available online 5 February 2014

### Keywords:

Indium tin oxide

Microwave sintering

Zinc oxide

Densification

## ABSTRACT

ITO ceramics with full densities are difficult to achieve using conventional heating because of the volatilization property of both indium oxide ( $\text{In}_2\text{O}_3$ ) and tin oxide ( $\text{SnO}_2$ ) at high temperatures. In our present study, we proposed to use a ZnO-doped and microwave hybrid-sintering approach to prepare for ITO ceramics with full densities under normal atmospheric condition. The investigation on the effect of the content of ZnO on the densification and resistivity of the ITO ceramics showed that as the ZnO content increased, the relative density of the ceramics increased while the weight loss and grain size decreased. The resistivity of the ceramics initially decreased by increasing the ZnO content but increased when the content of ZnO was more than 9.09 wt.%. Employing this logic, a relative density approaching 99% of the theoretical density was obtained and the sintering time required was just 25 min. The obtained ITO ceramics were pure ITO phase and had the lowest resistivity and the relative density of 98.1% when the content of ZnO was 9.09 wt.%. This hybrid sintering approach might open a new avenue in the fabrication of ITO ceramics with high densities.

© 2014 The Ceramic Society of Japan and the Korean Ceramic Society. Production and hosting by Elsevier B.V. All rights reserved.

## 1. Introduction

ITO (Tin-doped indium oxide) films are widely used as transparent electrodes for display devices and transparent coatings for solar-energy heat mirrors due to its excellent properties such as high electrical conductivity ( $10^4 \Omega^{-1} \text{cm}^{-1}$ ) and high transparency (85–90%) to visible light [1,2]. Various methods can be used to fabricate ITO films; among them, magnetron sputtering is one of the best techniques, which utilizes ITO targets [3,4]. Studies show that the properties of sputtering targets can greatly influence sputtering efficiency and quality of the sputtered films [5]. Dense targets are advantageous for increasing deposition rate and obtaining a more stable resistivity of the deposited films [6]. However, the densification of ITO ceramics with near-to-theoretical density is

difficult to achieve because of the volatilization property of both indium oxide ( $\text{In}_2\text{O}_3$ ) and tin oxide ( $\text{SnO}_2$ ) at high temperatures. Normally, the relative density of sintered ITO ceramics obtained by using conventional sintering in air under normal atmospheric conditions is in the range of 62–65% [7]. To achieve more dense ITO ceramics, some approaches such as hot press, hot isostatic pressing (HIP) and pressureless sintering under pure oxygen conditions have been used [8]. Nevertheless, vacuum hot press and hot isostatic pressing (HIP) are very expensive and have low production efficiency while pressureless sintering under pure oxygen conditions takes more than 10 h from the temperature-rise period to the end of heat preservation and additionally, sintering in an oxidizing atmosphere is dangerous and requires an expensive and complex system.

Recently, microwave sintering has received increasing attention, because of its desirable advantages, such as reduced activation energy [9–12,17], lower sintering temperature [12,13], enhanced diffusion process [14–17], very rapid heating rate [18] and so on. Microwave heating is a process in which the materials can couple with microwaves, absorb the electromagnetic energy and then transform into heat within the sample volume itself [19–21]. This is quite different from the conventional methods where heat is generated by external heating elements and then is transferred to the samples via radiation, conduction and convection. It was reported that ITO ceramics has 98% relative density by microwave sintering at 1600 °C for 1.5 h under oxygen atmosphere. The sintering time of ITO was drastically decreased. However, as mentioned

\* Corresponding author. Fax: +86 28 87634649.

E-mail addresses: [j.wang63@gmail.com](mailto:j.wang63@gmail.com), [jwang@swjtu.cn](mailto:jwang@swjtu.cn) (J. Wang).

Peer review under responsibility of The Ceramic Society of Japan and the Korean Ceramic Society.



Production and hosting by Elsevier

above, sintering the ITO targets in pure oxygen environment is dangerous.

Furthermore, the addition of ZnO to ITO was used to increase the relative density of ITO using conventional sintering under normal atmospheric conditions and a density up to 92% has been achieved [22]. The study shows that the addition of ZnO into ITO has no any negative effect on the optical properties of the sputtered films at all [22–25].

Considering the advantages of ZnO-doped sintering and microwave sintering, in the present study, ITO ceramics would be sintered by a ZnO-doped and microwave hybrid sintering approach in air under normal atmospheric conditions and the effect of the amount of ZnO on the densification and resistivity of the ceramics would be investigated so that high-density ITO ceramics would be obtained.

## 2. Experimental procedure

### 2.1. Preparation of ITO green bodies

The powders of ITO (99.9%,  $\text{In}_2\text{O}_3\cdot\text{SnO}_2 = 9:1$  wt.%) and ZnO (AR 99.9%) were purchased from CNMC Ningxia Orient Group Co., Ltd., China and Sigma–Aldrich, USA, respectively.

ITO powders were mixed with ZnO powders, and the investigated weight percentage of which was 0%, 4.76%, 7.41%, 9.09% and 16.7%, respectively. An organic binder (3 wt.% of polyvinyl butyral (PVB) dissolved in ethanol) was added to improve the compacting behavior. The mixed powders were wet ball milled in ethanol in a PTFE jar using agate balls for 12 h, and then dried in an oven at 110 °C for 8 h and whetted in an agate mortar. After whetting, the obtained powders were uniaxially pressed at 300 MPa in a steel die into pellets (20 mm in diameter, ~4 mm in thickness). The compacted pellets were then annealed at 500 °C for 2 h to remove organic binder. All the pellets had green body densities with a range of 46–47% of TD.

### 2.2. Microwave sintering

Microwave sintering was carried out in a microwave furnace with a silicon carbide ceramic crucible and alumina insulation in it (MKE 0.8/2.45–0.6/5.8, Linn High Therm GmbH, Germany). The used microwave frequency and power were 2.45 Hz and 800 W, respectively. The temperature was measured using a pyrometer. Microwave heating lasted 25 min and then cooled down naturally. The maximum temperature was 1358 °C during the process of sintering.

### 2.3. Characterization

The densities of the obtained ITO ceramics were measured using the Archimedes method. The phases of the samples were examined by an X-ray diffractometer (XRD) (X pert Pro MPD, Philips, Netherlands). The microstructure and morphology of the ceramics were characterized by a scanning electron microscopy (SEM) (Quanta 200, Philips, Netherlands). The electrical resistivity was measured at room temperature using a Automatic Four-Point Probe device (Model 280, Four Dimensions Inc., USA).

## 3. Results and discussion

X-ray diffraction (XRD) patterns for the initial powders and the prepared ITO ceramics doped with various contents of ZnO are shown in Fig. 1. It can be seen that all the X-ray diffraction peaks for both the initial powders and the sintered samples doped with

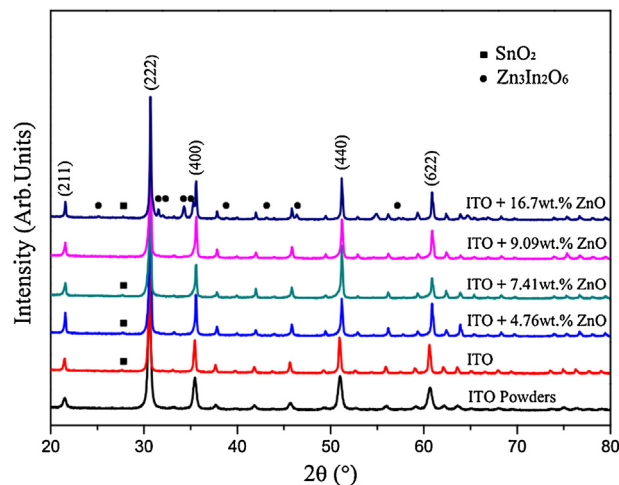


Fig. 1. XRD patterns for the initial ITO powders and the prepared ITO ceramics doped with various ZnO contents.

9.09 wt.% ZnO were indexed to the XRD patterns of the bixbyite structure of ITO (JCPDS File No. 89–4596). For the doped samples, no peaks corresponding to  $\text{ZnO}_x$  and  $\text{Zn}_k\text{In}_2\text{O}_{3+k}$  were observed while increasing ZnO content up to 9.09 wt.%. Nevertheless, some peaks corresponding to the phase of  $\text{Zn}_3\text{In}_2\text{O}_6$  could be detected in the sintered samples doped with 16.7 wt.% ZnO. Only the sintered samples doped with 9.09 wt.% ZnO among all the doped samples displayed pure ITO phase with a bixbyite structure, indicating that  $\text{Zn}^{2+}$  and  $\text{Sn}^{4+}$  substituted for  $\text{In}^{3+}$  within the  $\text{In}_2\text{O}_3$  lattice. In addition, some very weak characteristic peaks of  $\text{SnO}_2$  with a rutile structure were observed in the sintered samples doped with 0 wt.%, 4.76 wt.%, 7.41 wt.% and 16.7 wt.% ZnO, respectively. A systemic shift of the positions for (400), (440) and (622) peaks toward higher angle side of  $2\theta$  was observed in the samples doped with ZnO compared with pure ITO. The XRD peaks of ITO for the lattice planes with bigger absolute values of miller indices had a bigger shift toward high angle side of  $2\theta$  and that meanwhile, the more the ZnO content, the bigger the shift for the same XRD peaks of ITO. This kind of shift might be associated with a decrease in the lattice parameter caused by  $\text{Zn}^{2+}$  substitution [22].

Fig. 2 shows the images of the ITO ceramics sintered by using microwave sintering for 25 min in air and by using conventional sintering for 8 h in air. It can be seen that the sample sintered with conventional approach was still yellow in appearance whereas it was dark gray after microwave sintering, which was the same color like the targets for industrial use. It can be seen that the sample

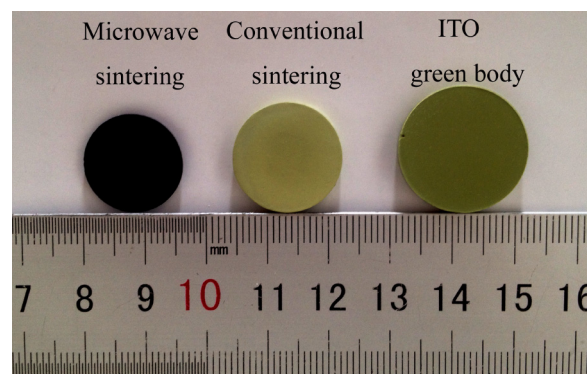
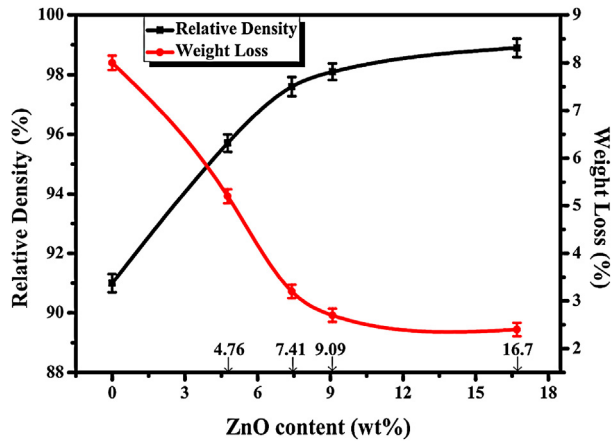


Fig. 2. Image of ITO ceramics before and after microwave sintering and conventional sintering.



**Fig. 3.** Relative densities and weight losses of the sintered ITO ceramics as a function of ZnO content.

sintered by microwave heating shrank at least 5 mm in diameter, compared with the unsintered ones. However, the sample sintered by conventional heating shrank only 2 mm in diameter.

The theoretical density and relative density of ZnO-doped ITO ceramics by microwave sintering for 25 min in air are shown in Table 1. From Table 1 and Fig. 3, it can be seen that the theoretical density of the ceramics decreased with increasing ZnO content due to the fact that the density of ZnO ( $5.606 \text{ g/cm}^3$ ) is smaller than ITO ( $7.15 \text{ g/cm}^3$ ). The relative density of the sintered samples increased with increasing ZnO content as has been expected. The samples without ZnO had the lowest relative density among all the sintered samples, which was 91.0% of the theoretical density. The highest relative density, approaching 99% of the theoretical density, was found in the samples doped with 16.7 wt.% ZnO.

In the meanwhile, it can be seen that the weight loss of the sintered bodies also changed with increasing the ZnO content in Fig. 3. It decreased with increasing the ZnO content. A large amount of weight loss was found when the doped relative amount of ZnO was less than 9.09 wt.%. Once when the doped relative amount of ZnO was more than 9.09 wt.% did the weight loss curve of the sintered bodies as function of the doped relative amount of ZnO become flat. From the relative density curve of the sintered bodies as a function of the doped relative amount of ZnO in Fig. 3, it can be seen that the lower the weight loss of the sintered bodies, the higher the relative density of the sintered bodies, and vice versa.

SEM examination was used to investigate the microstructures of the fractured surfaces of the sintered ITO ceramics and the average grain size was determined using the linear intercept method. Both the core and edge sections of the fracture surfaces of the sintered ITO ceramics with various ZnO contents are shown in Fig. 4. All the ITO ceramics sintered with the microwave heating approach presented a uniform distribution of pores and grains. It can be noted that there were lots of grains with transcrystalline ruptures on the fracture surfaces in the sintered ITO ceramics doped with high content of ZnO while they were not found on the fracture surfaces in sintered ITO ceramics doped without ZnO and with low content of ZnO, indicating that there would have been a high bond strength of

boundaries for the sintered ITO ceramics doped with high content of ZnO. The sintered ITO ceramics containing ZnO presented denser structures compared with the sintered ITO ceramics without ZnO. It can be seen that some pores with a size of about  $3\text{--}5 \mu\text{m}$  existed at boundaries for the sintered ITO ceramics doped without ZnO while they were seldom found in the sintered ITO ceramics doped with ZnO, especially when the content of ZnO was high. It can also be seen that all the sintered ITO ceramics displayed uniform grain size cross the whole fracture surfaces. A systemic decrease in grain size was found as ZnO content increased as shown in Fig. 4 and Table 1. The average grain size was  $8.54 \mu\text{m}$  for the sintered ITO ceramics without ZnO while it was between  $5.16 \mu\text{m}$  and  $6.96 \mu\text{m}$  for the sintered ITO ceramics doped with ZnO.

In order to compare with the microstructures of the ITO samples sintered with conventional approach, SEM micrographs of the fractured surfaces of the ITO ceramics sintered at  $1450^\circ\text{C}$  with conventional approach were shown in Fig. 5. It can be seen that the ITO ceramics sintered with conventional approach displayed an uneven distribution of pores and grains from the edge to the center. Densification presented a gradient structure with a dense edge but a porous core in sintered ITO ceramics. As expected, small grains existed in the cores. However, it can be noted that large grains were not detected in the edge sections but in the middle sections of ITO ceramics. Obviously, two different microstructures caused by two different sintering methods were associated with two different densification mechanisms. This will be discussed later.

Fig. 6 shows electrical resistivity of ITO ceramics versus the ZnO content. Resistivity presented a decreasing tendency as the content of ZnO increased before the content reached 16.7 wt.%. This might be associated with densification and grain size, because high densification and small grain size and hence more boundaries can improve charge transport. As a result, the electrical resistivity of ITO would be reduced due to the improvement of charge transport. When the content of ZnO was more than 9.09 wt.%, densification and grain size would not change significantly as shown in Fig. 4 and Table 1. However, due to higher electrical resistivity for ZnO compared with ITO, the increased content of ZnO would result in an increase of electrical resistivity of ITO as detected in the ITO ceramics doped with 16.7 wt.% ZnO.

Normally, densification and microstructures are generally determined by heating methods and temperature profiles caused by them. However, for the materials which have a property of volatilization at high temperatures, such as indium oxide and tin oxide, densification and microstructures are not only affected by heating methods and temperature profiles but also controlled by volatilization. Volatilization results in a decrease in densification and retards grain growth, thus leading to an inverse effect on densification and grain growth.

Because the direction of mass transport for densification caused by conventional heating is the opposite of volatilization in Fig. 7(a), it is difficult for materials with a very high sintering temperature and a property of volatilization to achieve high densification. As a result, conventional heating leads to a structure with a dense shell and a porous core for these materials during sintering as shown Fig. 7(a).

Compared with conventional heating which relies on thermal conduction and radiation to transport heat from the surface of

**Table 1**  
Relative densities and average grain sizes of the microwave-sintered ITO ceramics with various ZnO contents.

ZnO content	0 wt.%	4.76 wt.%	7.41 wt.%	9.09 wt.%	16.7 wt.%
Theoretical density ( $\text{g/cm}^3$ ) of ZnO-doped ITO ceramics	7.15	7.05	7.01	6.98	6.84
Relative density	(91.0 $\pm$ 0.25)%	(95.7 $\pm$ 0.25)%	(97.6 $\pm$ 0.30)%	(98.1 $\pm$ 0.25)%	(98.7 $\pm$ 0.30)%
Average grain size ( $\mu\text{m}$ )	8.54 $\pm$ 0.61	6.96 $\pm$ 0.55	5.87 $\pm$ 0.50	5.28 $\pm$ 0.46	5.16 $\pm$ 0.59



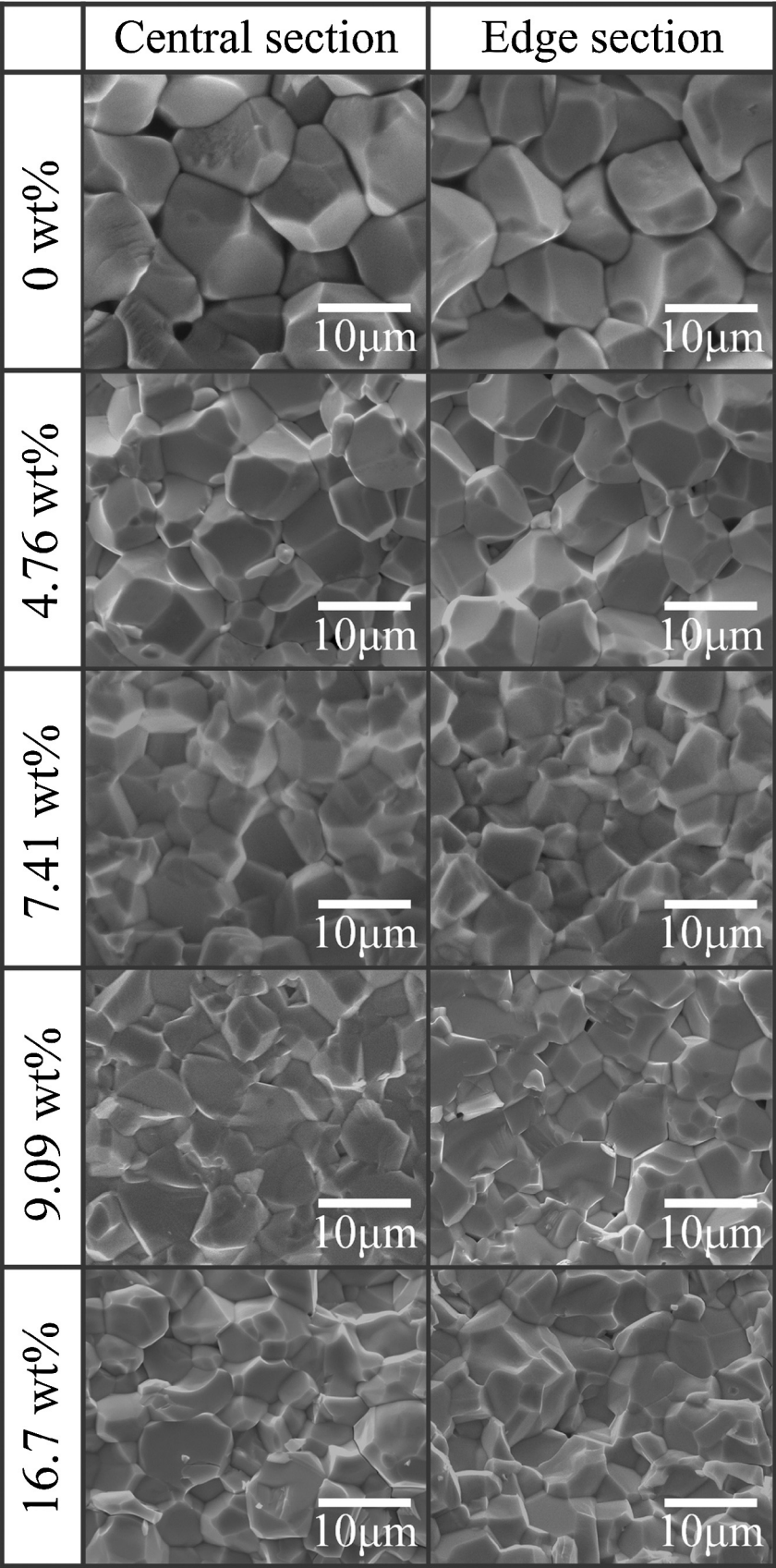


**Fig. 4.** SEM micrographs of the fractured surfaces (edge and central sections) of the microwave-sintered ITO ceramics with various ZnO contents: 0 wt.%, 4.76 wt.%, 7.41 wt.%, 9.09 wt.% and 16.7 wt.%.

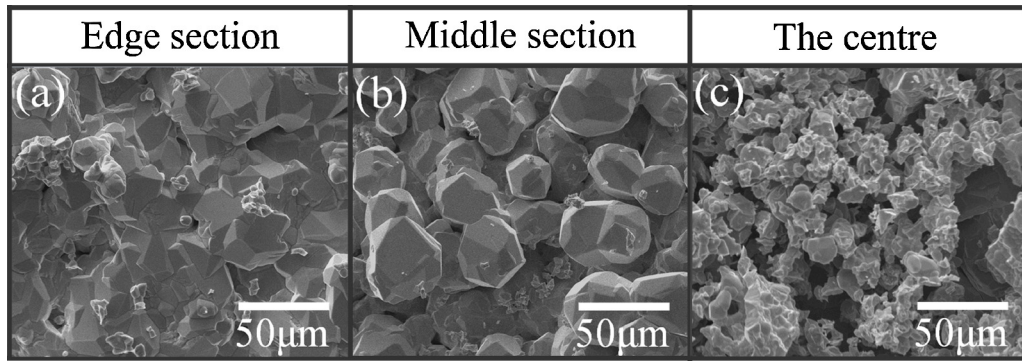


**Fig. 5.** SEM micrographs of a fractured surface of the ITO ceramics sintered at 1450 °C for 8 h using conventional heating: (a) edge section, (b) middle section, and (c) the center.

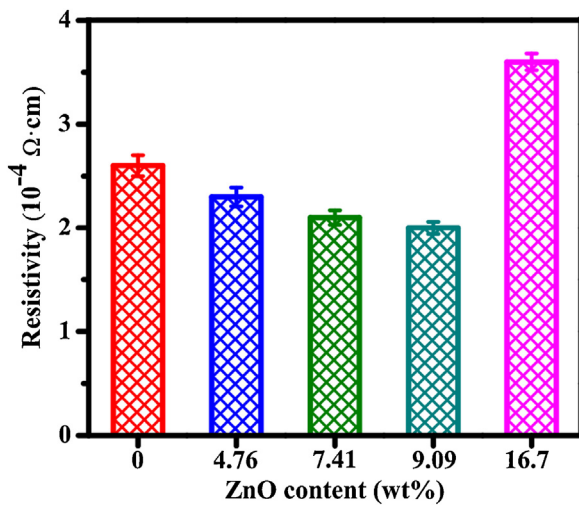


**Fig. 6.** Resistivity of the sintered ITO ceramics versus ZnO content.

the ceramic to the center of the body, because a distinguishing feature of microwave heating is its volumetric nature caused by direct depositing into the ceramic via the interaction between microwaves and materials, it can result in the creation of an inverse temperature profile with time, i.e. a hotter interior than

the surface because the surrounding air remains cooler than in the body [14,26,27]. This inverse temperature profile allows the densification direction to be the same with the volatilization direction in Fig. 7(b); hence, it is easier to remove pores out of sintered bodies compared with conventional sintering. It is possible for materials to achieve full density by using microwave heating if the level of microwave power is high enough to allow the “microwave effect” [13,18,26,28] to create a much higher rate for densification in a short sintering time than that for volatilization. However, it is still difficult to achieve full density only by using pure microwave heating under a low level of microwave power.

The obtained relative density reached 91% only for the ceramics sintered by microwave sintering under the low level of microwave power (800 W), while there was a significant increase in density compared with conventional sintering. A similar result was also obtained and the obtained relative density was 92% when only ZnO-doped sintering was used [22]. The 92% density seems to be the limiting value of the relative density obtained via a single approach whatever it is conventional sintering or pure microwave sintering under a low level of microwave power and or ZnO-doped sintering. In our present study, a hybrid approach, combining microwave sintering with ZnO-doped sintering, was used to achieve high densification. Because it combined the advantages of both microwave sintering and ZnO-doped sintering, an ITO ceramic material with a relative density of 98.7% has been obtained. Obviously, the hybrid approach has a large advantage over conventional sintering or pure

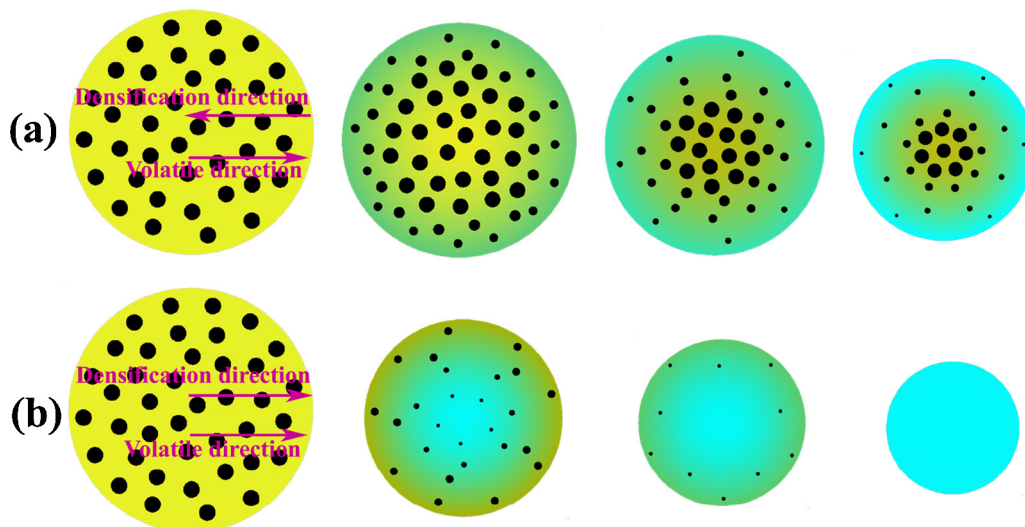


**Fig. 7.** Schematic diagram showing possible densification process and direction during conventional sintering (a) and microwave sintering (b). The black dots represent the pores in the samples, whereas yellow represents the region with low density and green the one with high density.

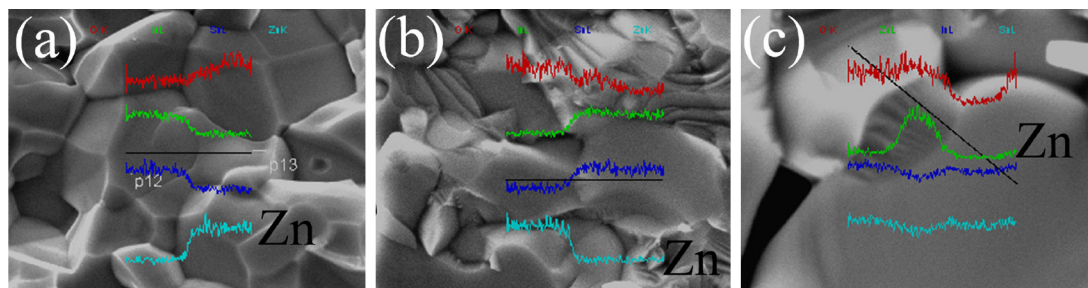


Fig. 8. Linear EDS analysis showing Zn dispersed at ITO grain boundaries or between ITO grains.

microwave sintering under a low level of microwave power and or ZnO-doped sintering. We think that the doped ZnO might play a crucial role on inhibiting the volatilization of In and Sn and grain growth during sintering. This has been proved by the fact that grain size decreases and density increases with increasing ZnO content. Linear EDS analysis and XRD analysis showed that Zn in the form of ZnO or  $\text{Zn}_k\text{In}_2\text{O}_{3+k}$  was dispersed at ITO grain boundaries or between ITO grains in Fig. 8, which could inhibit the volatilization of In and Sn and also would retard grain growth efficaciously. This effect became more pronounced with increasing the ZnO content.

Compared with microwave sintering, during conventional sintering process, due to the volatilization of components In and Sn consisting of ITO at high temperatures, they kept moving out of the sintered bodies to the exterior surfaces. As the amount of the volatilized In and Sn increased, they would redeposit on the surfaces and reformed grains on the surfaces via a process of classical nucleation and crystal growth. In the meanwhile, due to the volatilization of components In and Sn consisting of ITO, the grains in the center sections of sintered bodies became smaller and smaller with the volatilization and the pores got bigger and bigger. As a result, conventional heating led also to a microstructure with small grains in the edge sections and smaller small grains in the center sections and big grains in the middle sections as shown in Fig. 5.

The microwave processing of ceramics has been demonstrated to enhance sintering and grain growth. The enhanced mass transport and solid state reaction rates during the processing of a variety of ceramic, glass, polymer, and other organic and inorganic materials, including lower sintering or reaction temperatures, as well as accelerated kinetics for a wide range of processes in these materials and reduced activation energies, and these two aspects have broadly been called the “microwave effect”. The latter may therefore be categorized as a “nonthermal” phenomenon. According to the theory of the so-called ponderomotive driving forces [29], microwaves can induce an additional (electric) driving force, which specifies an enhanced diffusion in ionic solids. Freeman et al. [30] published the results of conductivity measurements made on sodium chloride single crystals under microwave and non-microwave conditions. Their results indicated that it was the driving force for diffusion that was enhanced by the application of microwaves. Similar conclusions were drawn by Wroe and Rowley [31] in their UK-based study on the sintering of partially stabilized zirconia. They found that an enhancement in densification when using microwaves was consistent with a dependence on the electric field experienced by the material. Both these experimental results support the ponderomotive theory first suggested by Rybakov and Semenov [29]. Additionally, previous studies by Birnboim et al. [32] showed the very strong influence of the ceramic particle-to-particle and grain boundary geometry and properties on the overall permittivity. This suggests that the local electric fields can be disproportionately strong in certain regions such as interparticle contact zones, pores, and rough grain surfaces [32]. For the two touching spheres model, the internal peak field in

the neck region can be much larger than the average field in the material, up to 10 times that of the externally applied field. The field in the neck region can be even higher, up to 30 times larger than the applied field. The net result is that the local absorbed energy in this region can be some 500 times larger than the average absorbed energy [32]. The results from Wang et al. [26] can fit this theory well, which showed that the most pronounced effect occurred during the intermediate stage of sintering, which is when the neck region dominates densification, and their results demonstrate clearly the effect of particle size on the magnitude of the effect. As predicted by the ponderomotive theory, finer particles, which will have smaller and more neck regions, show an enhanced microwave effect compared to larger particles. Their results generally showed that higher microwave power levels, finer particle sizes, and, particularly, greater microwave absorption can result in greater enhancement [26]. Wang et al. [26] study also indicated that, as a good microwave absorption material, ZnO was seen to have a great “microwave effect” in microwave sintering.

In the present study, the experiment results show that both factors of dopant of ZnO and “microwave effect” played a crucial role on enhancing the densification of ITO ceramics. For the first factor, it has been widely accepted that dopant may enhance the densification mechanism if suitable additives are chosen. In the study of the influence of  $\text{TiO}_2$  additives on the sintering behavior of  $\text{In}_2\text{O}_3$ , Nadaud et al. found that  $\text{TiO}_2$  doping caused an increase of sintering density and limited grain growth acting by a second-phase mechanism and also hindering the decomposition rate of  $\text{In}_2\text{O}_3$  by means of precipitation of  $\text{TiO}_2$  at the grain boundary, thus resulting in increased grain boundary diffusion at reduced diffusion activation energies [33]. In our present study, the enhancement mechanism of ZnO should be similar as described before. Another factor is microwave effect, which might also be correlated to the dopant of ZnO in the present study. The presence of  $\text{Zn}^{2+}$  in substitutional positions can lead to the formation of defects like oxygen vacancies. The following reaction could describe a possible formation process of oxygen vacancies:



Accompanied by the formation of interstitial atoms and vacancies, each interstitial-vacancy pair or double-vacancy point defect can be regarded as a polarized dipole, its damped vibration can lead to dielectric losses, then causing the absorption of microwave [34], which is beneficial for the “microwave effect” in sintering and hence for the enhancement of densification. As a result, ZnO doping will enhance the “microwave effect” and further promote the densification of ITO in sintering. According to the results from Wang et al. that higher microwave power levels, finer particle sizes, and, particularly, greater microwave absorption can result in greater enhancement, it can be expected that high densification can be achieved even when the content of ZnO additive is decreased if higher microwave power levels and finer particles are used.



#### 4. Conclusion

ITO ceramics with high density and low electrical resistivity were successfully fabricated by a ZnO-doped and microwave sintering approach under normal atmospheric condition. The sintering time required was just 25 min for full densification. The effect of the content of ZnO on the densification and resistivity of the ceramics has been investigated. As the ZnO content increased, the relative density of the ceramics increased while the weight loss and grain size decreased. The resistivity of the ceramics initially decreased with increasing the ZnO content but increased when the content of ZnO was more than 9.09%. The obtained ITO ceramics were pure ITO phase and had the lowest resistivity and the relative density of 98.1% when the content of ZnO was 9.09%. The highest relative density, approaching 99% of the theoretical density, was found in the samples doped with 16.7 wt.% ZnO. This hybrid sintering approach might provide a new route for the fabrication of ITO ceramics with high densities.

#### Acknowledgements

This work was supported by Scientific and Technical Supporting Program of Sichuan, China (2011GZ0139) and the Fundamental Scientific Research Funds for Central Universities, China (SWJTU11CX058).

#### References

- [1] P. Chandana, Udawatte and K. Yanagisawa, *J. Am. Ceram. Soc.*, 84, 251–253 (2001).
- [2] S.H. Brewer and S. Franzen, *J. Alloys Compd.*, 338, 73–79 (2002).
- [3] Y. Ye, L. Song, X. Song and T. Zhang, *J. Alloys Compd.*, 581, 133–138 (2013).
- [4] S. Ray, R. Banerjee, N. Basu, A.K. Batabyal and A.K. Barua, *J. Appl. Phys.*, 54, 3497–3501 (1983).
- [5] K. Utsumi and O. Matsnaga, *Thin Solid Films*, 334, 30–34 (1988).
- [6] T. Takeuchi, H. Kageyama, H. Nakazawa, T. Atsumi, S. Tamura, N. Kamijo, A. Takeuchi and Y. Suzuki, *J. Am. Ceram. Soc.*, 91, 2495–2500 (2008).
- [7] C.P. Udawatte and K. Yanagisawa, *J. Solid State Chem.*, 154, 444–450 (2000).
- [8] K. Nakajima and N. Sato, U.S. Patent US5094787 (1992).
- [9] M.A. Janney and H.D. Kimrey, *Mater. Res. Soc. Proc.*, 189, 215–227 (1991).
- [10] M.A. Janney, H.D. Kimrey, M.A. Schmidtdand and J.O. Kiggans, *J. Am. Ceram. Soc.*, 74, 1675–1681 (1991).
- [11] D.A. Lewis, *Mater. Res. Soc. Proc.*, 269, 21–31 (1992).
- [12] J. Luo, Z. Zhong and J. Xu, *Mater. Res. Bull.*, 47, 4283–4285 (2012).
- [13] M.A. Janney, C.L. Calhoun and H.D. Kimrey, *Ceram. Trans.*, 21, 311–318 (1991).
- [14] M. Oghbaei and O. Mirzaee, *J. Alloys Compd.*, 494, 175–189 (2010).
- [15] K.H. Brosnan, G.L. Messing and D.K. Agrawal, *J. Am. Ceram. Soc.*, 86, 1307–1312 (2003).
- [16] S.A. Freeman, J.H. Booske and R.F. Cooper, *Phys. Rev. Lett.*, 74, 2042–2045 (1995).
- [17] R. Raj, M. Cologna and J.S.C. Francis, *J. Am. Ceram. Soc.*, 94, 1941–1965 (2011).
- [18] K.I. Rybakov, E.A. Olevsky and E.V. Krikun, *J. Am. Ceram. Soc.*, 96, 1003–1020 (2013).
- [19] Y.V. Bykov, K.I. Rybakov and V.E. Semenov, *J. Phys. D: Appl. Phys.*, 34, R55–R75 (2001).
- [20] J. Cheng, D. Agrawal, Y. Zhang and R. Roy, *J. Mater. Sci. Lett.*, 20, 77–79 (2001).
- [21] J.H. Booske, R.F. Cooper and I. Dobson, *J. Mater. Res.*, 7, 495–501 (1992).
- [22] I. Saadeddin, H.S. Hilal, R. Decourt, G. Campet and B. Pecquenard, *Solid State Sci.*, 14, 914–919 (2012).
- [23] E. Fortunato, A. Pimentel, A. Gonçalves, A. Marques and R. Martins, *Thin Solid Films*, 502, 104–107 (2006).
- [24] N. Naghavi, A. Rougier, C. Marcel, C. Guéry, J.B. Leriche and J.M. Tarascon, *Thin Solid Films*, 360, 233–240 (2000).
- [25] T. Minami, T. Yamamoto, Y. Toda and T. Miyata, *Thin Solid Films*, 373, 189–194 (2000).
- [26] J. Wang, J. Binner and B. Vaidhyanathan, *J. Am. Ceram. Soc.*, 89, 1977–1984 (2006).
- [27] J. Binner, J. Wang and B. Vaidhyanathan, *J. Am. Ceram. Soc.*, 90, 2693–2697 (2007).
- [28] K.I. Rybakov, E.A. Olevsky and V.E. Semenov, *Scripta Mater.*, 66, 1049–1052 (2012).
- [29] K.I. Rybakov and V.E. Semenov, *Phys. Rev. B*, 49, (1) 64–68 (1994).
- [30] S.A. Freeman, J.H. Booske, R.F. Cooper and B. Meng, *Mater. Res. Soc. Proc.*, 347, 479–485 (1994).
- [31] F.C.R. Wroe and A.T. Rowley, *Ceram. Trans.*, 59, 69–76 (1995).
- [32] A. Birnboim, J.P. Calame and Y. Carmel, *J. Appl. Phys.*, 85, 478–482 (1999).
- [33] N. Nadaud, D. Kim and P. Boch, *J. Am. Ceram. Soc.*, 80, (5) 1208–1212 (1997).
- [34] D.M. Pozar, *Microwave Engineering*, Wiley, New York (1998).